HHS Public Access

Author manuscript

Oncogene. Author manuscript; available in PMC 2017 January 24.

Published in final edited form as:

Oncogene. 2016 September 08; 35(36): 4698–4707. doi:10.1038/onc.2016.11.

EGFR-targeted mAb therapy modulates autophagy in head and neck squamous cell carcinoma through NLRX1-TUFM protein complex

Yu Lei[1,†], **Benjamin A. Kansy**[1], **Jing Li**[1], **Linhai Cong**[1], **Yang Liu**[1], **Sumita Trivedi**[1], **Haitao Wen**[2], **Jenny P.-Y. Ting**[3], **Hongjiao Ouyang**[4], and **Robert L. Ferris**[1,5,*]

[1]Department of Otolaryngology, University of Pittsburgh Cancer Institute, School of Medicine, University of Pittsburgh, PA 15213

[2]Department of Surgery, Lineberger Comprehensive Cancer Center, School of Medicine, University of North Carolina, Chapel Hill, 27599

[3]Department of Microbiology and Immunology, Lineberger Comprehensive Cancer Center, School of Medicine, University of North Carolina, Chapel Hill, 27599

[4]Department of Restorative Dentistry and Comprehensive Care, School of Dental Medicine, University of Pittsburgh, Pittsburgh, PA 15213

[5]Department of Immunology, School of Medicine, University of Pittsburgh, PA 15213

Abstract

EGFR-targeted therapy in head and neck squamous cell carcinoma (HNSCC) patients frequently results in tumor resistance to treatment. Autophagy is an emerging underlying resistance mechanism, however, the molecular autophagy machinery in HNSCC cells and potential biomarkers of patient response to EGFR-targeted therapy remain insufficiently characterized. Here we show that the EGFR blocking with cetuximab leads to varied autophagic responses, which modulate cancer cell susceptibility to EGFR inhibition. Inhibition of autophagy sensitizes HNSCC cells to EGFR blockade. Importantly, we identify a novel signaling hub centering on the NLRX1-TUFM protein complex, promoting autophagic flux. Defects in the expression of either NLRX1 or TUFM result in compromised autophagy when treated with EGFR inhibitors. As a previously undefined autophagy-promoting mechanism, we found that TUFM serves as a novel anchorage site, recruiting Beclin-1 to mitochondria, promoting its polyubiquitination, and interfering with its interaction with Rubicon. This protein complex is also essential for endoplasmic reticulum (ER) stress signaling induction, possibly as an additional mechanism to promote autophagy. Utilizing tumor specimens from a novel neoadjuvant clinical trial, we show that increased expression of the autophagy adaptor protein, SQSTM1/p62, is associated with poor response to cetuximab therapy.

[*]To whom correspondence should be addressed: Robert L. Ferris, MD, PhD, FACS, ferrisrl@upmc.edu, Telephone: 412-623-0327, Fax: 412-623-4840, Address: 5117 Centre Avenue, Suite 2.26, Pittsburgh, PA 15213-1863.

[†]Present Address: Department of Periodontics and Oral Medicine, School of Dentistry; Department of Otolaryngology – Head and Neck Surgery, School of Medicine; Translational Oncology Program and Distributed Health Technologies; U-M Comprehensive Cancer Center, University of Michigan, Ann Arbor, MI 48109

These findings expand our understanding of the components involved in HNSCC autophagy machinery that responds to EGFR inhibitors, and suggest potential combinatorial approaches to enhance its therapeutic efficacy.

Keywords

EGFR; head and neck cancer; autophagy; cetuximab; NLRX1; TUFM

Introduction

Despite multimodality treatment, the 5-year survival of patients with head and neck squamous cell carcinoma (HNSCC) remains at less than 50% [1, 2]. A unique biologic property of HNSCC is that >90% of these tumors overexpress EGFR, which is pivotal in both tumor initiation and maintenance[3]. Thus in 2006, the FDA approved cetuximab, an EGFR monoclonal antibody, for the treatment of advanced or metastatic HNSCC and colorectal cancer, which also overexpresses EGFR. Cetuximab shows significant benefit in a subset of HNSCC patients, although the response rate is usually below 20% [4, 5]. Substantial effort has been invested to investigate the potential mechanisms and biomarkers that were associated with this treatment. However, neither FcγRIIIa polymorphism of natural killer (NK) cells, which affects their binding affinity with cetuximab, nor the EGFR expression or gene copy number in tumor cells were associated with HNSCC patient response [3, 6]. Overall, resistance mechanism associated with EGFR inhibitors remains poorly understood.

One potential contributing resistance mechanism is autophagy, an evolutionarily conserved physiologic process that eliminates and recycles excessive protein aggregates and damaged organelles to sustain nutrient supply and provides an intrinsic stress-responsive protective mechanism [7, 8]. Autophagy endows cancer cells with enhanced adaptability to endoplasmic reticulum (ER), oxidative, and metabolic stresses [9, 10]. Cetuximab promotes autophagy in lung cancer cells [11, 12], and strategic inhibition of autophagy could lead to therapeutic improvement [10, 11]. Also in line with this notion is an observation from a recent clinical trial, in which an ER stress- and autophagy- promoting agent bortezomib promoted early tumor progression in HNSCC patients when combined with cetuximab [13]. However, whether autophagy may have an impact on HNSCC cells response to direct EGFR inhibition and how EGFR signaling engages autophagy machinery in HNSCC cells remain unanswered questions.

We recently discovered a novel autophagy-promoting mitochondrial protein complex that relies on “nucleotide-binding, lots of leucine-rich repeats-containing protein member X1” (NLRX1) [14, 15]. NLRX1 belongs to an evolutionarily conserved NLR family that is potent at modulating cell death, inflammation, metabolism, and autophagy pathways [15–19]. Previously, we found that NLRX1 recruited the autophagy-related (ATG)12–ATG5 conjugate and ATG16L1 to mitochondria, through an intermediary partner Tu translation elongation factor mitochondrial (TUFM). Deficiency in NLRX1 or TUFM protein expression resulted in a severe defect in autophagy induction upon viral infection [15]. The

role of this multimeric protein complex in regulating cancer cell autophagic response is not known.

As a signaling converging point of nutrients sensing and intracellular stress signaling, autophagy may also synergize with other signaling adaptor molecules to promote tumorigenesis. A defect in SQSTM1/p62 expression was shown to impair tumor growth in vivo [20], and overexpression of p62 resulted in an increase in xenograft tumor mass [21]. In oral squamous cell carcinoma, cytoplasmic p62 expression level was significantly higher than normal mucosa, and cytoplasmic p62 level positively correlated with LC3B puncta, an autophagy induction marker [22]. Therefore, we evaluated whether EGFR-targeted therapy promoted autophagy and how EGFR signaling blockade engaged the autophagic machinery in HNSCC cells. Utilizing unique tumor specimens from a neoadjuvant cetuximab clinical trial, we also assessed whether the expression level of p62 was correlated with patient response to cetuximab treatment.

Results

EGFR-targeted therapy promoted autophagy in HNSCC cells

First, we screened a series of HNSCC cell lines to assess their autophagic induction upon cetuximab treatment. The conversion of LC3B-I to LC3B-II, reflective of autophagic induction, was monitored by immunoblot as previously described [15, 23]. The relative LC3B-II level to β-actin loading control was used to quantify autophagy induction. We found that cetuximab increased the LC3B-II/β-actin ratio in human papillomavirus (HPV)-negative PCI-13 cells and HPV-positive UDSCC2 and SCC90 cells, but autophagy induction in HPV-negative UMSCC22b cells was modest (Fig. 1A). To rule out the possibility that increased LC3B-II might be a result of decreased degradation, we treated two sensitive cell lines PCI-13 and UDSCC2 with chloroquine to assess the effect of cetuximab on autophagic flux. We found that cetuximab treatment induced autophagic flux in the presence of chloroquine (Fig. S1A–B). In order to confirm that the autophagy induction was due to inhibition of EGFR signaling, we treated the panel of HNSCC cell lines with an EGFR tyrosine kinase inhibitor, gefitinib, and found a similar autophagy induction profile. PCI-13, UDSCC2, and SCC90 cells showed increased LC3B-II/β actin ratio, while the autophagic induction in UMSCC22b cells was modest (Fig. 1B). As another technique to assess blockade of EGFR signaling-initiated autophagy response, we employed confocal imaging analysis. PCI-13 cells were first transfected with a plasmid expressing EGFP-LC3B 48hrs prior to treatment, and then these cells were challenged with cetuximab, gefitinib, or everolimus for 5hrs. EGFP-LC3B showed a weak diffuse cytoplasmic staining in the basal state with few punctate structure in the cytosol. The formation of LC3B puncta marks the induction of autophagy. In PCI-13 cells, cetuximab and gefitinib both induced puncta formation, similar to everolimus-treated (positive control) cells (Fig. 1C–D).

Inhibition of autophagy enhances EGFR inhibition-mediated cell growth arrest in HNSCC cells

In HNSCC cell lines, treatment with cetuximab alone only had modest to moderate inhibitory effects on proliferation in an XTT assay (Fig. 2A–D). These cells showed varied

sensitivity to chloroquine, which blocks the acidification of lysosomal compartment and the turnover of proteins delivered through autophagosomes. PCI-13, SCC90, and UMSCC22b cells appeared to be sensitive to chloroquine treatment alone (Fig. 2A, C, D). Importantly, combining chloroquine with cetuximab, which only showed modest effects in suppressing cancer cell proliferation, resulted in significantly greater growth inhibition in cells displaying autophagy induction upon cetuximab treatment (Fig. 2A–C). In UMSCC22b cells, which showed only modest autophagy induction by cetuximab treatment (Fig. 1A), combining cetuximab with chloroquine did not show a greater suppression of cancer cell proliferation compared to a single agent alone (Fig. 2D).

Although conferring potent autophagy inhibition, chloroquine also interferes with autophagy-independent lysosomal functions. In order to specifically interrogate the role of autophagy in promoting resistance to EGFR signaling blockade, we employed a recently identified, specific and potent autophagy inhibitor spautin-1, which specifically promotes the degradation of the Beclin-1-Vps34 autophagy-promoting protein complex [24]. PCI-13 and UDSCC2 cells, in which autophagy was induced with EGFR signaling blockade, were incubated with cetuximab or gefitinib, in the presence or absence of spautin-1. Gefitinib alone showed significant inhibitory effect on tumor cell proliferation (Fig 2F, H). Cetuximab did not show apparent growth-inhibitory effect when used as a single agent, but EGFR inhibitor plus spautin-1 demonstrated significantly stronger suppression of tumor cells proliferation than EGFR inhibitors alone (Fig. 2E–H). In addition, by combining spautin-1 with cetuximab, the clonogenic potential of PCI-13 and UDSCC2 cells was more severely compromised than either single agent treatment (Fig. S2A–D).

NLRX1 promotes cetuximab-induced autophagy and ER stress signaling

In order to understand how EGFR signaling blockade promotes autophagy in HNSCC cells, we employed a loss-of-function approach to examine the role of a unique mitochondrial protein complex. Recently, we discovered that the mitochondrial NLR protein, NLRX1, served as a critical tether point to recruit ATG12–ATG5 conjugate and ATG16L1, and promoted autophagy in multiple cell types in response to viral insults [14, 15]. We investigated whether NLRX1 was also pivotal for cetuximab-induced autophagy in HNSCC cells. In agreement with our previous finding of its wide tissue and cell type distribution profile [25], we found that NLRX1 was expressed by all tested HNSCC cell types. Interestingly, NLRX1 expression in UMSCC22b cells, which did not show robust autophagic induction upon EGFR signaling blockade, was lower compared to the other three tested HNSCC cell lines (Fig. 3A). As a confirmatory study, we knocked down the expression of NLRX1 in autophagy-inducible PCI-13 cells with a pool of 4 different siRNA sequences targeting different regions of NLRX1 mRNA, as previously described [25]. Under this condition, a severe defect in the generation of LC3B-II was observed in NLRX1-deficient cells compared to control cells transfected with a pool of 4 non-targeting siRNA sequences, suggesting that NLRX1 was indispensable for cetuximab-induced autophagy (Fig. 3B). To confirm that NLRX1 was modulating autophagic flux induced by cetuximab, we treated PCI-13 cells of normal or reduced expression level of NLRX1 with chloroquine to block the lysosomal degradation of LC3B-II. We showed cetuximab induced autophagic flux, and reduction of NLRX1 compromised the conversion of LC3B-I to LC3B-II (Fig. 3B).

To further understand how NLRX1 engages the autophagy machinery in HNSCC cells, we investigated whether NLRX1 promoted cetuximab-induced autophagy through ER stress signaling, which has a strong potential in promoting autophagy induction [26]. The phosphorylation of the eukaryotic initiation factor 2α (eIF2α) marks the induction of ER stress signaling and the activation of the unfolded protein response (UPR). We found that cetuximab induced the phosphorylation of eIF2α at the serine 51 residue more prominently at 5hrs post-treatment (Fig. 3C). Consistently, gefitinib treatment also potently promoted UPR as shown by phospoho-eIF2α immunoblotting (Fig. 3D), suggesting that the inhibition of the EGFR signaling pathway could trigger an UPR response. Notably, when we knocked down NLRX1 in PCI-13 cells, cetuximab-induced phosphorylation of eIF2α was abrogated, lending support to the critical role of NLRX1 in ER stress signaling, which serves as an underpinning mechanism for autophagy induction.

NLRX1-TUFM complex recruits Beclin-1 to mitochondria, facilitating its polyubiquitination

A recent report of EGFR-associated autophagy suppression showed that active EGFR regulates Beclin-1 interactome and promoted its interaction with inhibitors [27]. In addition, polyubiquitination of Beclin-1 was found to be critical for autophagy induction [28]. In two recent studies, NLRX1 was found to associate with the E3 ligase TRAF6 [29, 30]. Thus we examined whether the NLRX1-TUFM complex intersects with the Beclin-1 signaling and promotes its polyubiquitination in HNSCC cells. First, HA-Beclin-1 plasmid was transfected into PCI-13 cells, followed by immunoprecipitation (IP) of HA and immunoblotting of endogenous ubiquitin. We found cetuximab treatment promoted the polyubiquitination of Beclin-1 (Fig. 4A). Interestingly, upon autophagy induction, Beclin-1 was gradually recruited to TUFM, starting as early as 30min post-treatment, and more prominently after 2hrs (Fig. 4A). In agreement with our previous finding, under the stringent IP and wash conditions, we could not detect direct interaction between NLRX1 and Beclin-1 (Fig. 4A). To confirm our biochemical results, we performed a co-IP experiment in a completely endogenous setting, and recapitulated similar results (Fig. 4B). As the NLRX1-TUFM complex resides in mitochondria, we examined whether its interaction with Beclin-1 also occurs in mitochondria. Although some co-localization of Beclin-1 to mitochondria was seen in non-treated cells, we found more Beclin-1 was temporarily localized to mitochondria upon cetuximab treatment (Fig. 4C), suggesting that TUFM may provide a novel anchorage site for Beclin-1 to be localized to mitochondria.

TUFM mediates EGFR signaling blockade-induced autophagy and UPR

Since TUFM was found to be a member of the Beclin-1 interactome upon autophagy induction, we specifically investigated the function of TUFM in EGFR-mediated autophagy modulation. Using the same targeting construct that we previously used [15], we generated a lentivirus carrying a turboRFP marker and shRNA targeting TUFM to enforce high efficiency gene depletion. We transduced PCI-13 cells with this lentivirus (Fig. 5A), and selected the top 20% brightest population to generate a stable TUFM-deficient HNSCC cell line. We treated control and TUFM-deficient PCI-13 cells with cetuximab (Fig. 5B) or gefitinib (Fig. 5C), and showed that EGFR signaling blockade-induced autophagy as early as 2hrs post-treatment, and autophagy returned to basal level 24hrs after treatment. A defect in TUFM severely compromised autophagy induction by cetuximab or gefitinib, as evidenced

by a failure of LC3B-II production (Fig. 5B–C). In the presence of chloroquine, inhibition of EGFR signaling using either cetuxiamb or gefitinib promoted autophagic flux, and suppression of TUFM expression severely dampened this response (Fig. S3).

Notably, with a phenotype similar to NLRX1-deficient cells, TUFM-deficient cells exhibited a dampened UPR upregulation when treated with EGFR signaling inhibitors cetuximab or gefitinib (Fig. 5D–E). Considering the involvement of Beclin-1 in EGFR-associated autophagy regulation and TUFM-Beclin-1 interaction, we transfected control and TUFM-deficient cells with HA-Beclin-1, and immunoprecipitated HA-Beclin-1, followed by immunoblotting of endogenous ubiquitin. We found that gefitinib, similar to cetuximab, promoted the polyubiquitination of Beclin-1, and a reduction of TUFM expression level also inhibited the polyubiquitination of Beclin-1 (Fig. 5F). A recent study has revealed that EGFR signaling modulates the interaction between Beclin-1 and an inhibitor of autophagy Rubicon [27]. In order to directly test the hypothesis that whether TUFM regulates autophagy by engaging the Beclin-1-Rubicon complex, we immunoprecipitated endogenous Beclin-1 after challenging PCI-13 cells of normal or reduced expression levels of TUFM with gefitinib. In agreement with the previous study [27], we found Rubicon gradually dissociated from the Beclin-1 complex through the course of gefitinib treatment, however, such dynamics was disturbed when TUFM expression was knocked down despite of comparable amount of immunoprecipitated Beclin-1 protein (Fig. 5G). Thus, we identified a novel mechanism that regulates EGFR blockade-induced autophagy, namely that NLRX1 and TUFM form a mitochondrial protein complex, which mediates UPR signaling, recruits Beclin-1, and impedes Beclin-1 interaction with Rubicon, to intersect with autophagy machinery in HNSCC cells (Fig. 5H). As an important mechanism that cetuximab employs to impose an anti-tumor effect, this mAb engages CD16 on NK cells to promote immunogenic cytotoxicity [31], and autophagy has emerged as a critical regulator of tumor cell sensitivity to immunogenic attack [32]. Thus we reasoned that Beclin-1-TUFM complex may promote tumor cell resistance to NK cells through autophagy. We added cetuximab and NK cells into the culture of PCI-13 cells with or without expressing shRNA targeting Beclin-1 at the tumor : effector (T:E) ratio of 1:10, and incubated for 24hrs. Consistent with previous report [32], knocking down Beclin-1 potentiated cetuximab-induced, NK cells-mediated cytotoxicity (Figure S4A). Similarly, a reduction of TUFM expression also resulted increased tumor cell sensitivity to cetuximab-induced immunogenic attack (Figure S4B).

SQSTM1/p62 is associated with patient response to cetuximab

Recent evidence showed that cytoplasmic p62 expression correlated with LC3B puncta and was higher in oral squamous cell carcinoma than in normal oral mucosa [22]. High p62 level was also associated with a worse prognosis [22]. Thus we interrogated specimens procured from a neoadjuvant phase II clinical trial (NCT01218048), in which HNSCC patients were administered four weekly doses of cetuximab. Tumor tissue from 23 patients was procured before and after treatment. Demographics of enrolled patients are shown in supplementary Table 1. Based on our recent study using the same clinical trial material, this sample size is sufficient to provide statistically sound conclusions [33]. In representative paired tumor sections, the p62 expression level post-treatment showed varied response compared to pre-

treatment specimens (Fig. 6A). Aperio ImageScope quantitation tool was used to determine the staining scores of each core, and found that staining for p62 was significantly stronger in the post-treatment group (p=0.03) (Fig. 6B). Due to the small size of pre-treatment biopsy specimen, not all specimens were paired, and thus overall staining density for p62 was analyzed among the whole cohort. In the available paired tumors, p62 staining in the post-treatment group was also significantly elevated (p=0.04) (Fig. 6C). A head and neck radiologist scored paired contrast CT scans pre- and post- neoadjuvant cetuximab treatment to evaluate patient tumor burden and objective response to treatment. Notably, in agreement with previous work that p62 levels may be a marker for unfavorable prognosis [22], we found p62 staining levels were significantly higher after cetuximab treatment among poor clinical responders (p=0.03), whereas there was no p62 induction in good clinical responders (Fig. 6D).

Discussion

In this study, we demonstrated that EGFR-targeted treatment resulted in reproducible autophagy induction in some HNSCC cells. A combination of cetuximab or gefitinib with inhibitors of autophagy augmented suppression of proliferation in tumor cells with higher inducible autophagic response. Importantly, we revealed that NLRX1-TUFM protein complex actively recruited Beclin-1 to mitochondria, promoting its polyubiquitination. A defect in NLRX1-TUFM protein complex compromised the autophagy induction in cancer cells. The clinical importance of these findings was supported by the increased expression of the autophagy adaptor p62 among patients who responded poorly to cetuximab treatment, in a prospective cohort of HNSCC patients.

The role of autophagy in cancer initiation and treatment has been found to be context-dependent, because it may engage distinct signaling modules with contrasting functions at different stages of tumor initiation and development [9, 11]. As evidence has accumulated, autophagy appears to serve as a protective mechanism against tumor initiation. However, it could endow cancer cells with markedly increased adaptability to metabolic crisis when established solid tumors undergo treatment [9, 11]. In line with this evidence, the combination of cetuximab with an autophagy-promoting agent bortezomib to treat HNSCC patients resulted in early disease progression [13]. In our study, we showed that a combination of autophagy inhibitors, including a specific inhibitor that disrupts Beclin-1-associated Vps34 complex function, could potentiate EGFR inhibition-mediated growth suppression. This finding is also consistent with a recent study, in which non-small-cell lung carcinoma cells exhibited increased cell death with less autophagy and decreased cell death with enhanced autophagy [27]. Another mechanism that underlies the efficacy of cetuximab is it may also activate natural killer (NK) cells to launch immunogenic attack against tumor cells, recent findings showed autophagy could promote tumor cells resistance to NK-mediated killing mechanism [32], suggesting that targeting autophagy may benefit direct sensitization of tumor cells to EGFR inhibition and immunogenic killing.

Appreciating the pathologic significance of EGF signaling in many types of solid tumors, the mechanisms underlying EGFR inhibition-induced autophagy are rapidly emerging. Two groups indicated Beclin-1 and its interactome were involved EGFR-mediated autophagy

modulation [27, 34]. Active EGFR facilitated the phosphorylation of Beclin-1 and its binding to inhibitory molecules [27]. In addition, EGFR could also regulate the interaction between Beclin-1 and an autophagy inhibitor Rubicon [27]. These findings suggest the fundamental role of Beclin-1-interacting partners in modulating EGFR-mediated autophagy. In our study, we revealed a novel Beclin-1-interacting protein TUFM that promotes autophagy by promoting Beclin-1 polyubiquitination and interfering the Beclin-1:Rubicon interaction. Beclin-1 could be localized to mitochondria and interact with Bcl-2 and Bcl-x_L [35]. Interestingly, we found that TUFM could gradually associate with Beclin-1 after cetuximab treatment, suggesting that TUFM may provide an additional anchorage site for Beclin-1 mitochondrial localization. Mitochondria were noted to provide membrane for autophagosome biogenesis [36]. The fact that TUFM associates with both ATG12–ATG5-ATG16L1 complex and Beclin-1 suggests that TUFM may play an important role in promoting autophagosome biogenesis.

In addition to direct biochemical association with Beclin-1 and the ATG12–ATG5 complex, we also showed the NLRX1-TUFM complex linked increased intracellular stress to autophagy induction. NLRX1 is a unique NLR protein in that it is the only mitochondrial protein in this 22-member family. Besides its autophagy-promoting function, NLRX1 was also shown to mediate the generation of reactive oxygen species (ROS), and reduction of NLRX1 lead to lower ROS level [37]. ROS is a potent inducer of autophagy and UPR signaling [26]. In order to further delineate the mechanism underlying attenuated autophagy response in NLRX1-deficient HNSCC cells upon cetuximab challenge, we showed that NLRX1 was also essential for UPR activation. Activated UPR signaling could promote autophagy in an ATF4-dependent fashion [38]. ATF4 is responsible for establishing resistance to cetuximab treatment by inducing autophagy in multiple cancers [39–41]. Another critical target of PERK is eIF2α; and a non-phosphorylatable mutant (S51A) of eIF2α loses its capacity in inducing autophagy [42]. Our results suggest that NLRX1-TUFM complex could employ two different mechanisms, including engaging the Beclin-1 interactome and promoting UPR, to modulate cancer cell autophagy response.

Because HNSCC patients' response rate to cetuximab treatment is low, identification of biomarkers that are associated with clinical response may shed light to the development of co-targeting strategies. Procurement of specimens before and after cetuximab administration uniquely enabled us to assess whether autophagy signaling molecule could be associated with objective clinical response in cetuximab treated patients. We showed that tumor from poor responders exhibited stronger expression of p62. Although the level of p62 could decrease within hours during starvation-induced autophagy, it contains multiple domains that could engage complex signaling pathways, and its expression is also regulated by transcriptional mechanisms [23]. Thus, its expression level over a long period of time is confounded by transcriptional regulation. In fact, in several studies, p62 level was also found increased with enhanced autophagic flux [43, 44]. Further supporting this notion, only a limited number of LC3B puncta and lower cytoplasmic p62 was observed in normal oral mucosa, in comparison with much more increased LC3B puncta and cytoplasmic p62 staining levels in oral squamous cell carcinoma, and a high level of p62 was associated with a poor prognosis [22]. These results are conceptually consistent with our findings. But we also appreciate that p62 has complex functions including tumor growth-regulating potential

independent of autophagy-related mechanisms. The poor outcome associated with high p62 level may be also explained by a pro-survival NF-κB-dependent mechanism that could synergize with autophagy to promote tumor growth [20]. In addition, p62 could activate a protective antioxidant response by engaging the Keap1-Nrf2 signaling pathway and delivers resistance to chemotherapy [45]. Thus, the efficacy of co-targeting p62 in a cetuximab-based regimen warrants future investigation.

In summary, our study showed inhibition of autophagy sensitizes HNSCC cells to EGFR-targeted treatment, and identified that TUFM, a novel member of the Beclin-1 interactome, comprises a novel signaling hub, which connects EGFR inhibition, ER stress signaling, and autophagy induction in HNSCC cells. This study represents a conceptual advance in that the NLR family, traditionally thought to modulate inflammatory signaling in response to microbial challenges, may also directly modulate cancer cell susceptibility to treatment through an autophagy-dependent mechanism. Importantly, utilizing clinical HNSCC specimens, we found that increased level of the autophagy signaling adaptor p62 was associated with an unfavorable objective response. These results provide additional molecular candidates for developing potential co-targeting strategies to enhance an EGFR-targeted therapeutic regimen.

Materials and Methods

Cell culture and treatment

PCI-13, UDSCC2, SCC90, and UMSCC22b cells were maintained in complete DMEM medium supplemented with 10% fetal bovine serum (FBS), 4.5g/L glucose, 110mg/L sodium pyruvate, 2mM L-glutamine, 1% penicillin and 100μg/ml streptomycin. PCI-13 and SCC90 cells were developed and maintained at the University of Pittsburgh. UDSCC2 cells were provided by Dr. Henning Bier at the University of Düsseldorf. UMSCC22b was generated by Dr. Thomas Carey at the University of Michigan. All cell lines have been recently authenticated and tested for mycoplasma contamination. Cetuximab was provided by Bristol-Myers Squibb, NYC, NY. Gefitinib was reconstituted in DMSO (Cat. sc-202166, Santa Cruz Biotechnology). Everolimus was reconstituted according to manufacturer's instruction (Cat. 07741, Sigma-Aldrich).

RNAi-based protein expression knockdown and plasmid transfection

PCI13 cells were transfected with an ON-TARGETplus SMARTpool of 4 siRNA sequences targeting NLRX1 mRNA (Cat. L-012926-01-0005, Dharmacon Research Inc.) or a control pool of 4 non-targeting siRNA (Cat. D-001810-10-05, Dharmacon Research Inc.), using lipofectamine™ RNAiMax (Cat. 13778-150, Invitrogen). Plasmid expressing EGFP-LC3B (human) protein was obtained (Cat. 24920, Addgene), and transfected using PolyFect (Cat. 301105, Qiagen). In order to generate stable TUFM-deficient PCI-13 cells and non-targeting control cells, we purchased TripZ control construct bacteria stock (Cat. RHS4743, Thermo Scientific) and sh-TUFM construct bacteria stock (Oligo ID V2THS_222080, Cat. RHS4696-99362407, Thermo Scientific). Lentiviruses were packaged as previously described [46].

Western blots and co-immunoprecipitation

Cells were lysed in NP-40-based lysis buffer (1% NP-40, 50mM Tris-HCl pH8.0, 150mM NaCl) with freshly added complete protease inhibitor cocktail (Cat. 11873580001, Roche). Protein lysates were separated using 15% or 4–12% precast gels (Cat. 58504 and 58522, Lonza). The membranes were immunoblotted using the following antibodies: anti-LC3B (Cat. 2775, Cell Signaling), anti-NLRX1, anti-eIF2α (Cat. 9722, Cell Signaling), anti-Phospho-eIF2α (Ser51) (119A11) (Cat. 3597, Cell Signaling), anti-HA-HRP (Cat. 2999, Cell Signaling), anti-ubiquitin (Cat. 3936, Cell Signaling), anti-Beclin-1 (Cat. 3495, Cell Signaling), anti-p62 (Cat. Ab56416, Abcam), anti-TUFM (Cat. 67991, Abcam), Anti-Mouse kappa light chain (HRP) (Cat. ab99632, Abcam), anti-β-Actin (Cat. A5441, Sigma-Aldrich), anti-Rabbit IgG (H+L)-HRP Conjugate (Cat. W4011, Promega), and anti-mouse IgG (H+L), HRP Conjugate (Cat. 170-6516, Bio-Rad Laboratories). For semi-endogenous co-IP, whole cell lysates were incubated with HA-agarose beads (Cat. 26181, Thermo Scientific) at 4°C overnight, and then boiled in Laemmli's buffer at 95°C for 5 min. In the endogenous co-IP experiment, whole cell lysates were pre-cleared with protein A/G beads and incubated with Beclin-1 antibody overnight. The protein A/G UltraLink resin (Cat. 53132, Thermo Scientific) was added on the next day and incubated for 2 hrs. Resin were washed five times before boiling in the Laemmli's buffer.

Laser confocal imaging and colocalization analysis

PCI-13 cells were seeded on glass bottom microwell dishes (Cat. P35GCol-1.5-14-C, MatTek) 24hrs prior to transfection with pEGFP-LC3. Two days post-transfection, the cells were incubated with cetuximab, gefitinib, or everolimus for 5hrs. Live cells were examined under an Olympus FV1000 confocal microscope. The number of puncta per section was counted in 40 cells per group and in a total of 200 cells. In the colocalization experiment, PCI-13 cells were stained with MitoTracker Deep Red FM (Cat. M22426, Invitrogen) after indicated treatments. Cells were then fixed with 3.7% paraformaldehyde in pre-warmed complete medium for 15min at 37°C. Fixed cells were permeabilized in 0.2% Triton X-100 PBS for 15min on a shaker, and stained with anti-HA-Alexa Fluor 488 (Cat. A-21287, Life Technologies) overnight. The nuclei were counter-stained with DAPI (Cat. D1306, Life Technologies), prior to examination under the laser confocal microscope).

Patient recruitment and TMA analysis

The clinical trial was approved by IRB protocol #: MOD08090382-22/PRO08090382 at the University of Pittsburgh, and registered in the ClinicalTrials.gov (NCT01218048). Written informed consent was obtained after the nature and potential side effects of this treatment were explained to the patients. Patients exclusion criteria include: (1) Eastern Cooperative Oncology Group (ECOG) performance status beyond 1, (2) patients below 18 years of age, (3) female patients who are pregnant or breastfeeding, and (4) patients who have uncontrolled infection and cardiac disease. Tumor specimens prior to and after cetuximab treatment were sectioned and evaluated to ensure the tumor mass comprised at least 70% of the total potential core area. Two to three cores were extracted from each specimen, and built into a tissue microarray (TMA). Immunohistochemical stains were assessed using Aperio ImageScope. The staining score was calculated by multiplying staining density and percent

of positivity. The pathologist was blinded to the group allocation during the evaluation of the cores. Patients' radiographic response to cetuximab treatment was evaluated by a head and neck radiologist.

Statistical Analysis

Comparisons among different treatment groups were made by Kruskal–Wallis one-way analysis of variance (ANOVA) followed by *Bonferroni* multiple comparison tests. Comparisons between two groups were made using paired or unpaired t-test. A Bartlett test of homogeneity of variances among different groups was performed. Analyses were performed using Graphpad Prism 5.0 (Graphpad Software, Inc.). Bar graphs were presented as mean ± standard error of mean. A p value of less than 0.05 was considered significant.

Supplementary Material

Refer to Web version on PubMed Central for supplementary material.

Acknowledgments

Financial Support: K99 DE024173 (YL), T32 CA060397 (RLF), R01 DE019727 (RLF), P50 CA097190 (RLF), R01 CA182418 (HO), and R21 CA161150 (HO).

This work is supported by NIH grants K99 DE024173 (YL), T32 CA060397 (RLF), R01 DE019727 (RLF), P50 CA097190 (RLF), R01 CA182418 (HO), and R21 CA161150 (HO). The UPCI core facilities are supported in part by P30 CA047904. We thank Dr. Barton Branstetter for the interpretation of the radiographic findings of the enrolled patients.

References

1. Jemal A, Clegg LX, Ward E, Ries LA, Wu X, Jamison PM, et al. Annual report to the nation on the status of cancer, 1975–2001, with a special feature regarding survival. Cancer. 2004; 101:3–27. [PubMed: 15221985]
2. Edwards BK, Noone AM, Mariotto AB, Simard EP, Boscoe FP, Henley SJ, et al. Annual Report to the Nation on the status of cancer, 1975–2010, featuring prevalence of comorbidity and impact on survival among persons with lung, colorectal, breast, or prostate cancer. Cancer. 2013
3. Sharafinski ME, Ferris RL, Ferrone S, Grandis JR. Epidermal growth factor receptor targeted therapy of squamous cell carcinoma of the head and neck. Head & neck. 2010; 32:1412–1421. [PubMed: 20848399]
4. Reeves TD, Hill EG, Armeson KE, Gillespie MB. Cetuximab therapy for head and neck squamous cell carcinoma: a systematic review of the data. Otolaryngology--head and neck surgery : official journal of American Academy of Otolaryngology-Head and Neck Surgery. 2011; 144:676–684. [PubMed: 21493327]
5. Argiris A, Karamouzis MV, Raben D, Ferris RL. Head and neck cancer. Lancet. 2008; 371:1695–1709. [PubMed: 18486742]
6. Srivastava RM, Lee SC, Andrade Filho PA, Lord CA, Jie HB, Davidson C, et al. Cetuximab-activated natural killer (NK) and dendritic cells (DC) collaborate to trigger tumor antigen-specific T cell immunity in head and neck cancer patients. Clin Cancer Res. 2013
7. Rubinsztein DC, Codogno P, Levine B. Autophagy modulation as a potential therapeutic target for diverse diseases. Nature reviews Drug discovery. 2012; 11:709–730. [PubMed: 22935804]
8. Yang Z, Klionsky DJ. Eaten alive: a history of macroautophagy. Nature cell biology. 2010; 12:814–822. [PubMed: 20811353]
9. White E. Deconvoluting the context-dependent role for autophagy in cancer. Nature reviews Cancer. 2012; 12:401–410. [PubMed: 22534666]

10. Amaravadi RK, Lippincott-Schwartz J, Yin XM, Weiss WA, Takebe N, Timmer W, et al. Principles and current strategies for targeting autophagy for cancer treatment. Clin Cancer Res. 2011; 17:654–666. [PubMed: 21325294]
11. White E, DiPaola RS. The double-edged sword of autophagy modulation in cancer. Clin Cancer Res. 2009; 15:5308–5316. [PubMed: 19706824]
12. Li X, Fan Z. The epidermal growth factor receptor antibody cetuximab induces autophagy in cancer cells by downregulating HIF-1alpha and Bcl-2 and activating the beclin 1/hVps34 complex. Cancer research. 2010; 70:5942–5952. [PubMed: 20634405]
13. Argiris A, Duffy AG, Kummar S, Simone NL, Arai Y, Kim SW, et al. Early tumor progression associated with enhanced EGFR signaling with bortezomib, cetuximab, and radiotherapy for head and neck cancer. Clin Cancer Res. 2011; 17:5755–5764. [PubMed: 21750205]
14. Lei Y, Wen H, Ting JP. The NLR protein, NLRX1, and its partner, TUFM, reduce type I interferon, and enhance autophagy. Autophagy. 2013; 9:432–433. [PubMed: 23321557]
15. Lei Y, Wen H, Yu Y, Taxman DJ, Zhang L, Widman DG, et al. The mitochondrial proteins NLRX1 and TUFM form a complex that regulates type I interferon and autophagy. Immunity. 2012; 36:933–946. [PubMed: 22749352]
16. Ting JP, Willingham SB, Bergstralh DT. NLRs at the intersection of cell death and immunity. Nature reviews. 2008; 8:372–379.
17. Davis BK, Wen H, Ting JP. The Inflammasome NLRs in Immunity, Inflammation, and Associated Diseases. Annual review of immunology. 2011
18. Ting JP, Duncan JA, Lei Y. How the noninflammasome NLRs function in the innate immune system. Science (New York, NY. 2010; 327:286–290.
19. Wen H, Gris D, Lei Y, Jha S, Zhang L, Huang MT, et al. Fatty acid-induced NLRP3-ASC inflammasome activation interferes with insulin signaling. Nature immunology. 2011; 12:408–415. [PubMed: 21478880]
20. Wei H, Wang C, Croce CM, Guan JL. p62/SQSTM1 synergizes with autophagy for tumor growth in vivo. Genes & development. 2014; 28:1204–1216. [PubMed: 24888590]
21. Mathew R, Karp CM, Beaudoin B, Vuong N, Chen G, Chen HY, et al. Autophagy suppresses tumorigenesis through elimination of p62. Cell. 2009; 137:1062–1075. [PubMed: 19524509]
22. Liu JL, Chen FF, Lung J, Lo CH, Lee FH, Lu YC, et al. Prognostic significance of p62/SQSTM1 subcellular localization and LC3B in oral squamous cell carcinoma. British journal of cancer. 2014; 111:944–954. [PubMed: 24983366]
23. Klionsky DJ, Abdalla FC, Abeliovich H, Abraham RT, Acevedo-Arozena A, Adeli K, et al. Guidelines for the use and interpretation of assays for monitoring autophagy. Autophagy. 2012; 8:445–544. [PubMed: 22966490]
24. Liu J, Xia H, Kim M, Xu L, Li Y, Zhang L, et al. Beclin1 controls the levels of p53 by regulating the deubiquitination activity of USP10 and USP13. Cell. 2011; 147:223–234. [PubMed: 21962518]
25. Moore CB, Bergstralh DT, Duncan JA, Lei Y, Morrison TE, Zimmermann AG, et al. NLRX1 is a regulator of mitochondrial antiviral immunity. Nature. 2008; 451:573–577. [PubMed: 18200010]
26. Kroemer G, Marino G, Levine B. Autophagy and the integrated stress response. Molecular cell. 2010; 40:280–293. [PubMed: 20965422]
27. Wei Y, Zou Z, Becker N, Anderson M, Sumpter R, Xiao G, et al. EGFR-mediated Beclin 1 phosphorylation in autophagy suppression, tumor progression, and tumor chemoresistance. Cell. 2013; 154:1269–1284. [PubMed: 24034250]
28. Shi CS, Kehrl JH. TRAF6 and A20 regulate lysine 63-linked ubiquitination of Beclin-1 to control TLR4-induced autophagy. Science signaling. 2010; 3:ra42. [PubMed: 20501938]
29. Allen IC, Moore CB, Schneider M, Lei Y, Davis BK, Scull MA, et al. NLRX1 protein attenuates inflammatory responses to infection by interfering with the RIG-I-MAVS and TRAF6-NF-kappaB signaling pathways. Immunity. 2011; 34:854–865. [PubMed: 21703540]
30. Xia X, Cui J, Wang HY, Zhu L, Matsueda S, Wang Q, et al. NLRX1 negatively regulates TLR-induced NF-kappaB signaling by targeting TRAF6 and IKK. Immunity. 2011; 34:843–853. [PubMed: 21703539]

31. Lopez-Albaitero A, Lee SC, Morgan S, Grandis JR, Gooding WE, Ferrone S, et al. Role of polymorphic Fc gamma receptor IIIa and EGFR expression level in cetuximab mediated, NK cell dependent in vitro cytotoxicity of head and neck squamous cell carcinoma cells. Cancer immunology, immunotherapy : CII. 2009; 58:1853–1864. [PubMed: 19319529]
32. Baginska J, Viry E, Berchem G, Poli A, Noman MZ, van Moer K, et al. Granzyme B degradation by autophagy decreases tumor cell susceptibility to natural killer-mediated lysis under hypoxia. Proceedings of the National Academy of Sciences of the United States of America. 2013; 110:17450–17455. [PubMed: 24101526]
33. Jie HB, Schuler PJ, Lee SC, Srivastava RM, Argiris A, Ferrone S, et al. CTLA-4(+) Regulatory T Cells Increased in Cetuximab-Treated Head and Neck Cancer Patients Suppress NK Cell Cytotoxicity and Correlate with Poor Prognosis. Cancer research. 2015; 75:2200–2210. [PubMed: 25832655]
34. Tan X, Thapa N, Sun Y, Anderson RA. A kinase-independent role for EGF receptor in autophagy initiation. Cell. 2015; 160:145–160. [PubMed: 25594178]
35. Liang XH, Yu J, Brown K, Levine B. Beclin 1 contains a leucine-rich nuclear export signal that is required for its autophagy and tumor suppressor function. Cancer research. 2001; 61:3443–3449. [PubMed: 11309306]
36. Hailey DW, Rambold AS, Satpute-Krishnan P, Mitra K, Sougrat R, Kim PK, et al. Mitochondria supply membranes for autophagosome biogenesis during starvation. Cell. 2010; 141:656–667. [PubMed: 20478256]
37. Tattoli I, Carneiro LA, Jehanno M, Magalhaes JG, Shu Y, Philpott DJ, et al. NLRX1 is a mitochondrial NOD-like receptor that amplifies NF-kappaB and JNK pathways by inducing reactive oxygen species production. EMBO reports. 2008; 9:293–300. [PubMed: 18219313]
38. Rouschop KM, van den Beucken T, Dubois L, Niessen H, Bussink J, Savelkouls K, et al. The unfolded protein response protects human tumor cells during hypoxia through regulation of the autophagy genes MAP1LC3B and ATG5. The Journal of clinical investigation. 2010; 120:127–141. [PubMed: 20038797]
39. Zang Y, Thomas SM, Chan ET, Kirk CJ, Freilino ML, Delancey HM, et al. Carfilzomib and ONX 0912 Inhibit Cell Survival and Tumor Growth of Head and Neck Cancer and Their Activities are Enhanced by Suppression of Mcl-1 or Autophagy. Clin Cancer Res. 2012
40. Zang Y, Thomas SM, Chan ET, Kirk CJ, Freilino ML, Delancey HM, et al. The next generation proteasome inhibitors carfilzomib and oprozomib activate prosurvival autophagy via induction of the unfolded protein response and ATF4. Autophagy. 2012; 8
41. Milani M, Rzymski T, Mellor HR, Pike L, Bottini A, Generali D, et al. The role of ATF4 stabilization and autophagy in resistance of breast cancer cells treated with Bortezomib. Cancer research. 2009; 69:4415–4423. [PubMed: 19417138]
42. Talloczy Z, Jiang W, Virgin HWt, Leib DA, Scheuner D, Kaufman RJ, et al. Regulation of starvation- and virus-induced autophagy by the eIF2alpha kinase signaling pathway. Proceedings of the National Academy of Sciences of the United States of America. 2002; 99:190–195. [PubMed: 11756670]
43. Toepfer N, Childress C, Parikh A, Rukstalis D, Yang W. Atorvastatin induces autophagy in prostate cancer PC3 cells through activation of LC3 transcription. Cancer biology & therapy. 2011; 12:691–699. [PubMed: 21768780]
44. Colosetti P, Puissant A, Robert G, Luciano F, Jacquel A, Gounon P, et al. Autophagy is an important event for megakaryocytic differentiation of the chronic myelogenous leukemia K562 cell line. Autophagy. 2009; 5:1092–1098. [PubMed: 19786835]
45. Xia M, Yu H, Gu S, Xu Y, Su J, Li H, et al. p62/SQSTM1 is involved in cisplatin resistance in human ovarian cancer cells via the Keap1-Nrf2-ARE system. International journal of oncology. 2014; 45:2341–2348. [PubMed: 25269472]
46. Moore CB, Guthrie EH, Huang MT, Taxman DJ. Short hairpin RNA (shRNA): design, delivery, and assessment of gene knockdown. Methods in molecular biology. 2010; 629:141–158. [PubMed: 20387148]

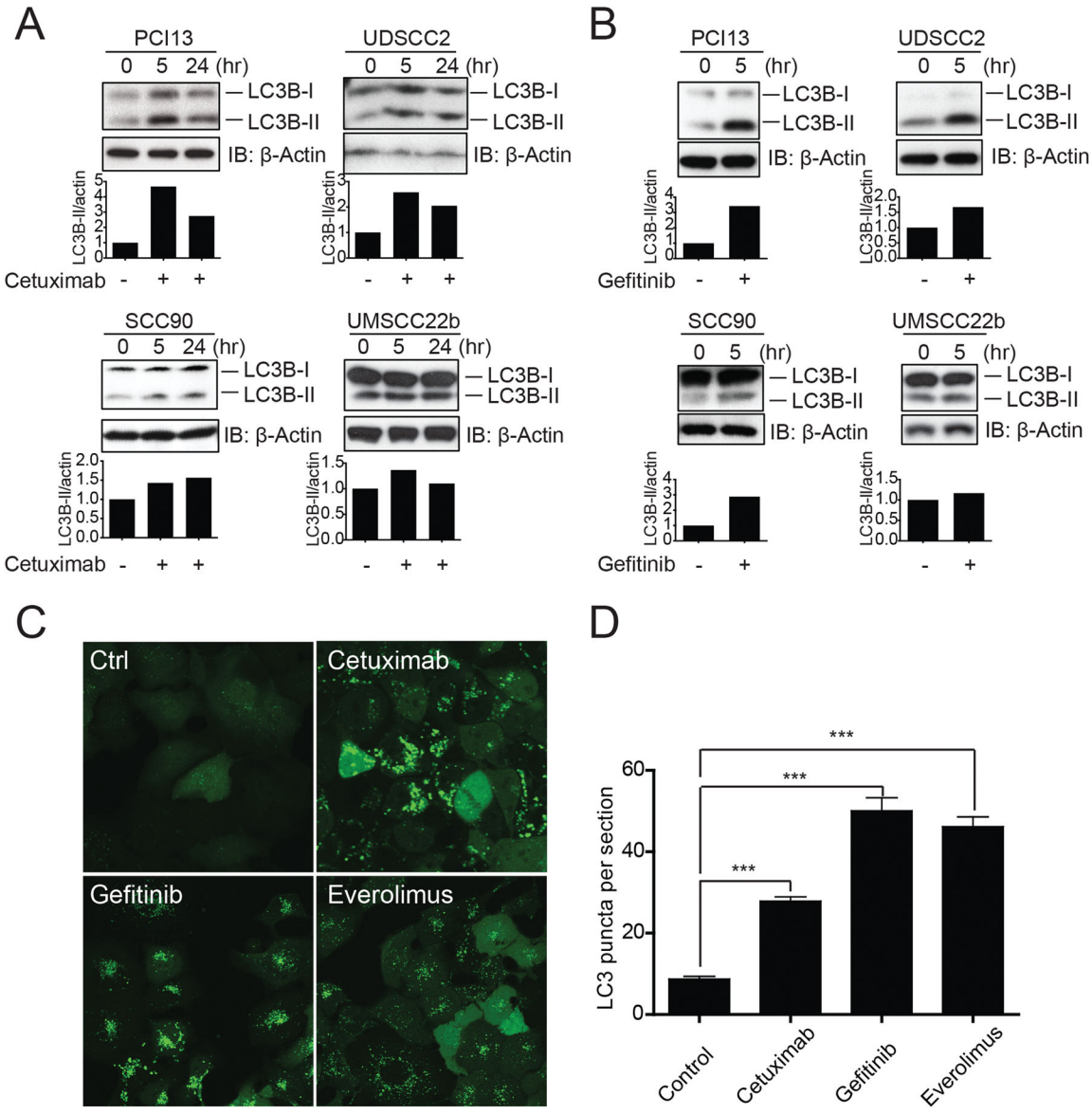

Fig. 1. Inhibition of EGFR signaling promotes autophagy

(A) PCI-13, UDSCC2, SCC90, and UMSCC22b cells were treated with 5.0μg/ml cetuximab for the indicated periods of time. Cell lysates were then subjected to SDS-PAGE and immunoblotting analysis of LC3B. The expression of β-actin was monitored as a loading control. Densitometry was performed using ImageJ. (B) PCI-13, UDSCC2, SCC90, and UMSCC22b cells were treated with 12.5μM gefitinib for 5hrs. Cell lysates were immunoblotted for LC3B and β-actin to examine autophagy induction. Densitometry was analyzed using ImageJ. (C) PCI-13 cells were transfected with EGFP-LC3B plasmids 48 hrs prior to treatments. After a visual confirmation of successful transfection of over 90% of cells under a fluorescence microscope, cells were then treated with PBS, 5.0μg/ml cetuximab, 12.5μM gefitinib, 100nM everolimus, and then examined using laser confocal microscopy. (D) Autophagic puncta were counted in one section of 40 cells from each group. Comparisons were made by one-way ANOVA followed by Bonferroni post-test.

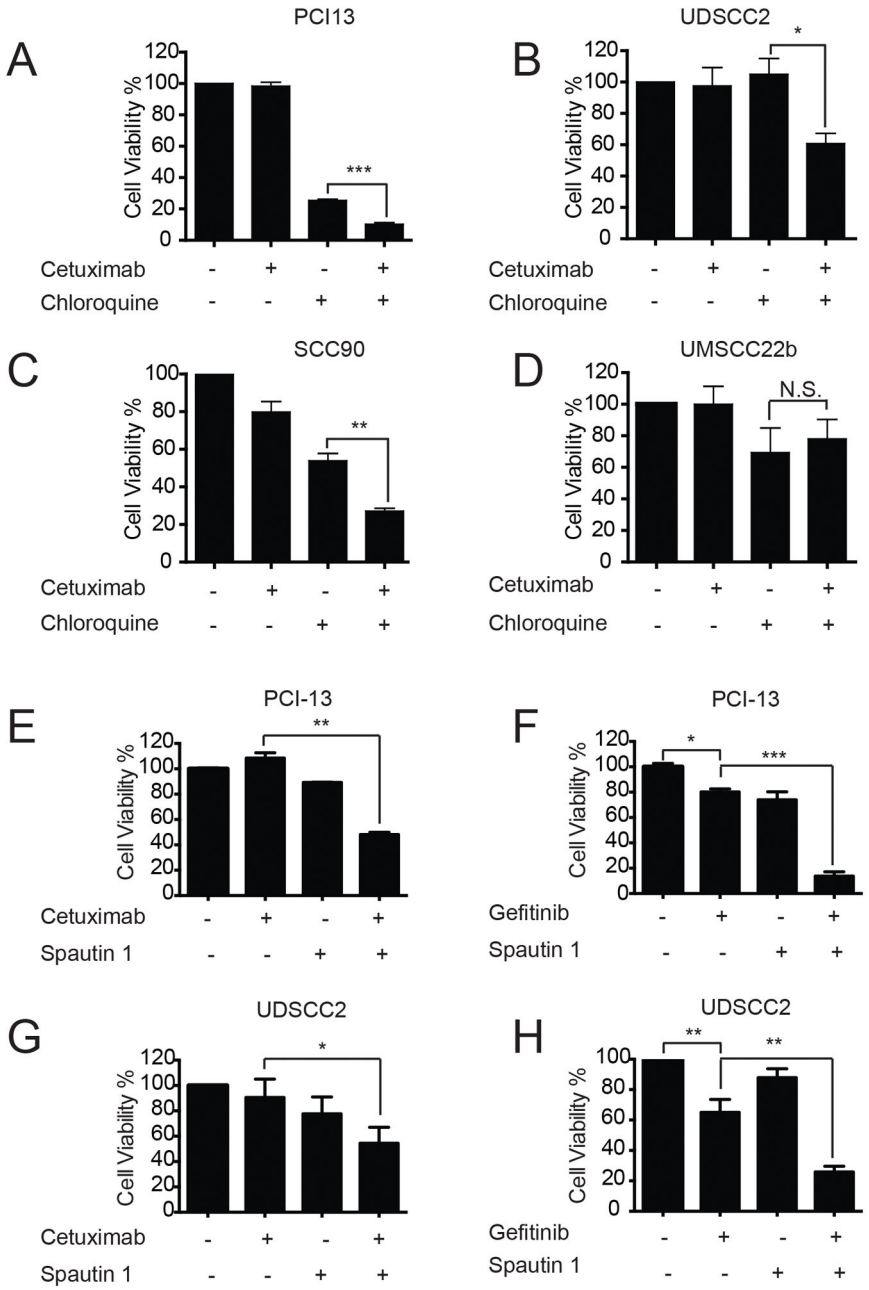

Fig. 2. Suppression of autophagy enhances the anti-proliferative effect of EGFR inhibitors in HNSCC cells

(A–D) PCI-13, UDSCC2, SCC90, and UMSCC22b cells were treated with cetuximab at 5.0μg/ml in the presence or absence of 100nM chloroquine. Cell proliferation was quantitated by XTT assays 5 days post-treatment. (E–F) PCI-13 cells were treated with 5.0μg/ml cetuximab or 12.5μM gefitinib in the presence or absence of 10μM spautin-1. (G–H) UDSCC2 cells were treated by 5.0μg/ml cetuximab or 12.5μM gefitinib with or without spautin-1. Cell proliferation was quantitated by XTT assays. Each group contained three biological replicates.

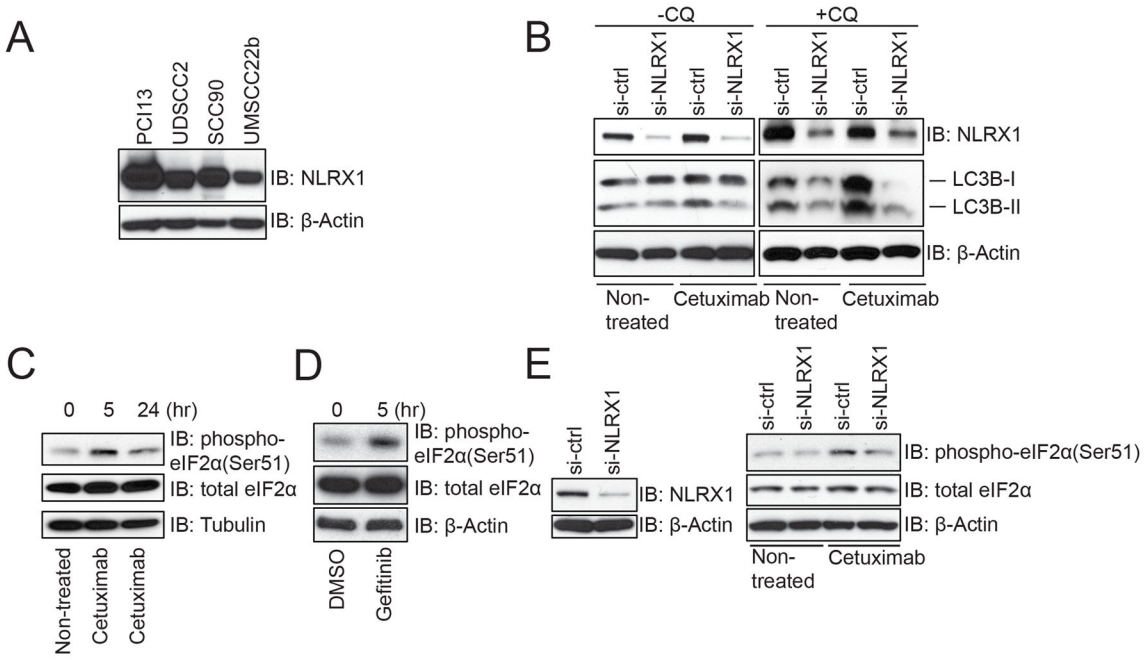

Fig. 3. NLRX1 promotes cetuximab-induced autophagy and ER stress signaling

(A) 1.0×10^6 non-treated HNSCC cells were lysed for immunoblotting against NLRX1. (B) PCI-13 cells were transfected with a pool of 4 NLRX1-targeting or non-targeting siRNAs 72 hours prior to incubation with 5.0μg/ml cetuximab for 5hrs in the presence or absence of a 2-hour incubation with 80μM chloroquine. Cell lysates were analyzed for LC3B. (C) PCI-13 cells were treated with 5.0μg/ml cetuximab and lysed for immunoblotting against the indicated ER stress markers. (D) PCI-13 cells were treated with 12.5μM gefitinib and lysed for immunoblotting against the indicated proteins. (E) PCI-13 cells were transfected with indicated pools of siRNAs, and then treated with cetuximab for immunoblotting of the indicated ER stress markers.

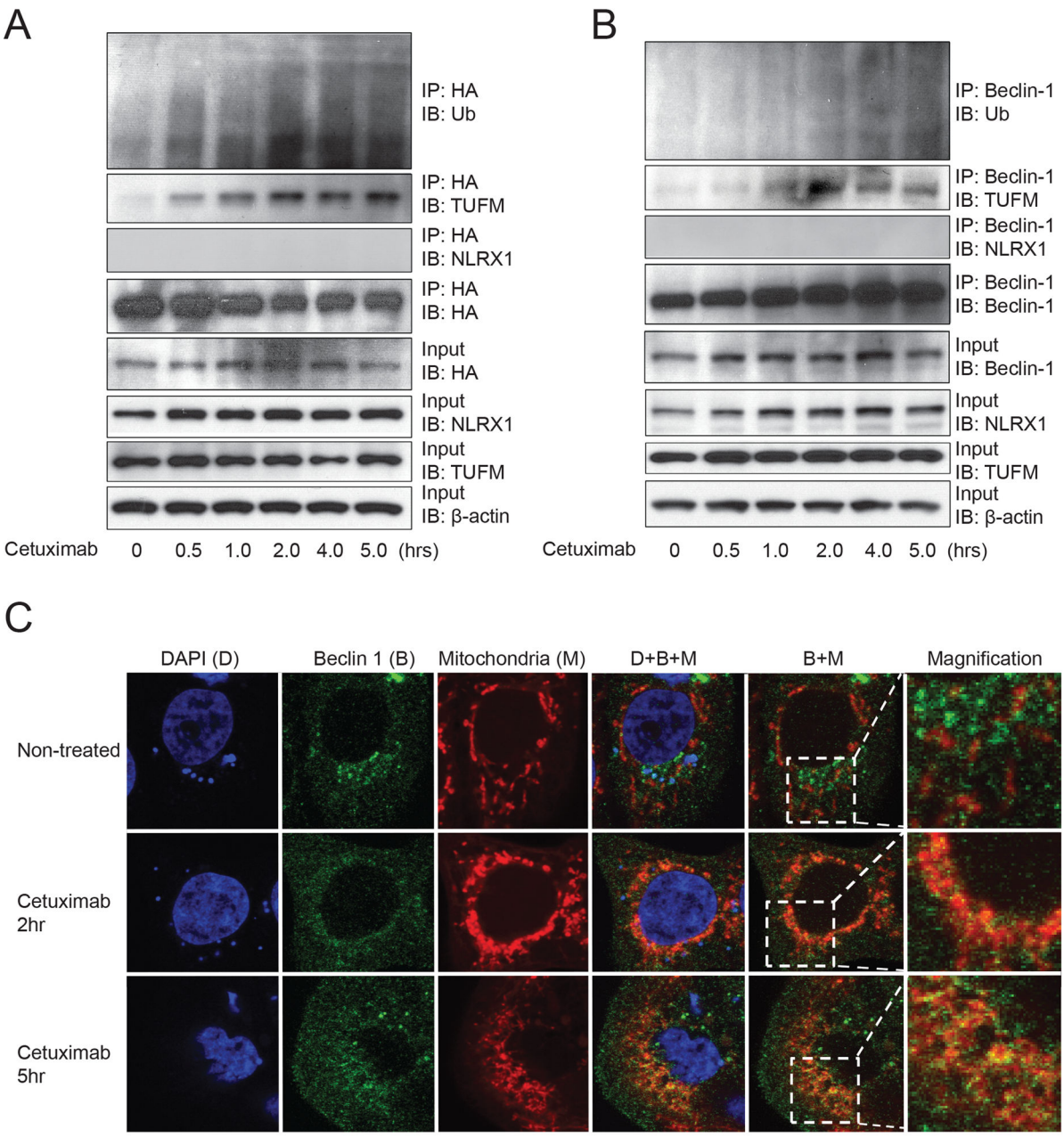

Fig. 4. NLRX1-TUFM complex recruits Beclin-1 to mitochondria, facilitating its polyubiquitination

(A) PCI-13 cells were transfected with HA-Beclin-1 plasmid, and treated with cetuximab 48hrs post-transfection. Cells were lysed and immunoprecipitated with HA-agarose beads, which were washed five times and boiled in Laemmli sample buffer. Pre-IP lysate control and IP samples were separated by SDS-PAGE and immunoblotted for the indicated proteins. (B) PCI-13 cells were lysed and pre-cleared before endogenous Beclin-1 complex was immunoprecipitated with protein A/G ultralink beads. Pre-IP input and IP samples were processed as described in (A). (C) PCI-13 cells were transfected with HA-Beclin-1 and treated with cetuximab for 2hrs and 5hrs, followed by a MitoTracker Deep Red FM staining.

Cells were then fixed, permeabilized, and stained with anti-HA-Alexa 488. The nuclei were counter-stained with DAPI on the next day prior to imaging. Images were captured using laser confocal microscopy.

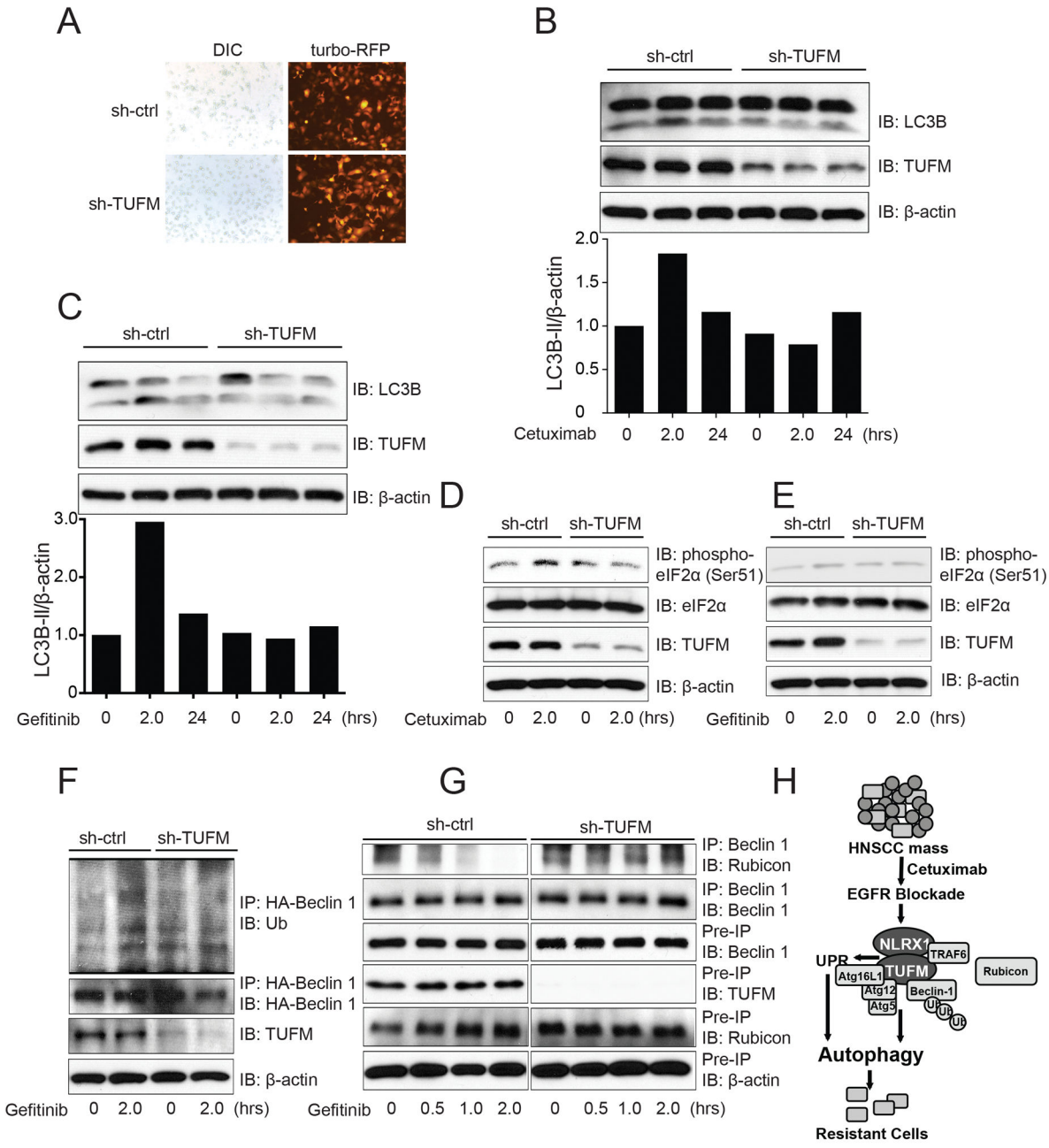

Fig. 5. TUFM mediates EGFR signaling blockade-induced autophagy and UPR

(A) PCI-13 cells were transduced with lentiviruses containing a turbo-RFP expressing non-targeting construct or shRNA targeting TUFM. The brightest 20% cells were sorted out by FACS and used to establish stable knockdown cell lines. (B–C) Control and TUFM-deficient PCI-13 cells were treated with 5.0μg/ml cetuximab or 2.5μM gefitinib for 2hrs and 24hrs. Cell lysates were immunoblotted for LC3B, β-actin, and TUFM. Densitometry was performed using ImageJ. (D–E) Control and TUFM-deficient PCI-13 cells were treated with cetuximab or gefitinib for 2hrs. Cell lysates were immunoblotted with indicated ER stress markers and TUFM for knockdown control. (F) Control or TUFM knockdown PCI-13 cells

were treated with 2.5μM gefitinib for 2hrs. Cell lysates were immunoprecipitated with anti-HA-agarose beads, which were then washed 5 times and boiled in Laemmli sample buffer. Pre-IP lysate and IP were immunoblotted against the indicated proteins. (G) PCI-13 cells stably expressing shRNA targeting TUFM or control cells were treated with gefitinib for the indicated periods of time prior to immunoprecipitation of endogenous Beclin-1. Immunoprecipitated proteins were separated by SDS-PAGE, and immunoblotted for Rubicon and Beclin-1. Pre-IP lysates were immunoblotted for the indicated control inputs. (H) This schematic highlights a novel signaling hub centering on NLRX1-TUFM. Upon inhibition of EGFR signaling, TUFM interferes with the interaction between Beclin-1 and Rubicon, promotes Beclin-1 polyubiquitination, and induces UPR signaling to modulate autophagy. Induction of autophagy in HNSCC cells increases their resistance to EGFR inhibitors.

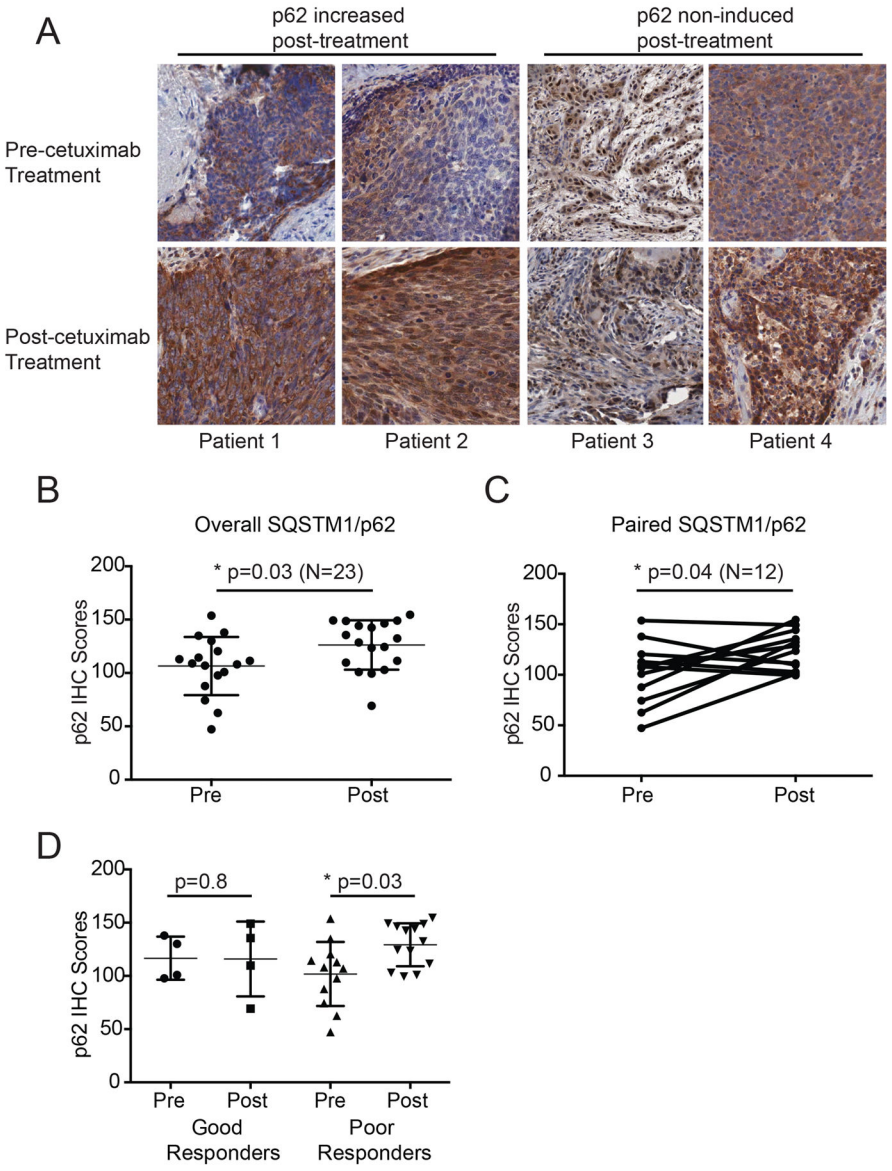

Fig. 6. SQSTM1/p62 induction is associated with resistance to cetuximab therapy

(A) In our single-agent phase II clinical trial, 4 weekly doses of cetuximab were administered in patients with stage III/IV HNSCC. Tumor specimens were procured before and after treatment and built into a TMA. Representative pictures from both groups showed varied p62 induction. (B) The IHC staining density was analyzed using Aperio ImageScope software, and IHC scores were recorded by averaging at least 2 cores from each specimen. IHC scores from all patients were recorded and compared between pre-treatment and post-treatment groups. (C) Only IHC scores of paired specimens from pre-treatment and post-treatment were compared. (D) Clinical response was evaluated by scoring tumor shrinkage, using paired pre- and post- contrast CT scans. The staining density of p62 was assessed in tumors from patients who responded favorably and those who responded poorly to cetuximab treatment.